Available online at www.sciencedirect.com
ScienceDirect
Developmental Biology 311 (2007) 11–24
DEVELOPMENTAL BIOLOGY
www.elsevier.com/developmentalbiology

Multiple cardiovascular defects caused by the absence of alternatively spliced segments of fibronectin

Sophie Astrof [1], Denise Crowley, Richard O. Hynes *

Howard Hughes Medical Institute, Center for Cancer Research, Department of Biology, Massachusetts Institute of Technology, Cambridge, MA, USA

Received for publication 16 May 2007; revised 6 July 2007; accepted 6 July 2007
Available online 12 July 2007

Abstract

Alternatively spliced variants of fibronectin (FN) containing exons EIIIA and EIIIB are expressed around newly forming vessels in development and disease but are downregulated in mature vasculature. The sequences and patterns of expression of these splice variants are highly conserved among vertebrates, suggestive of their biological importance; however the functions of EIIIA and EIIIB-containing FNs are unknown. To understand the role(s) of these splice variants, we deleted both EIIIA and EIIIB exons from the FN gene and observed embryonic lethality with incomplete penetrance by embryonic day 10.5. Deletion of both EIIIA and EIIIB exons did not affect synthesis or cell surface deposition of FN, indicating that embryonic lethality was due specifically to the absence of EIIIA and EIIIB exons from FN. *EIIIA/EIIIB double-null* embryos displayed multiple embryonic cardiovascular defects, including vascular hemorrhage, failure of remodeling embryonic and yolk sac vasculature, defective placental angiogenesis and heart defects. In addition, we observed defects in coverage and association with dorsal aortae of alpha-smooth-muscle-actin-positive cells. Our studies indicate that the presence or absence of EIIIA and EIIIB exons alters the function of FN and demonstrate the requirement for these alternatively spliced exons in cardiovascular development.

Keywords: Cardiovascular development; Fibronectin; Alternative splicing

Introduction

Organismal development, whether in invertebrates or vertebrates, involves extensive migration of cells and germ layers to generate the animal body plan. These migrations take place through a variety of adhesive cell–cell and cell–matrix interactions. Extracellular matrix provides both adhesive and signaling platforms for the migrating cells, (reviewed in Hynes, 1990; Hynes, 2002; Lauffenburger and Horwitz, 1996; Schwartz et al., 1995). While many extracellular matrix molecules such as laminins and collagens appeared early in evolution and are conserved from fly to human, fibronectin (FN) has been found only in vertebrates and its appearance in evolution correlates with the appearance of organisms with endothelial cell-lined vasculature (Hynes and Zhao, 2000; Whittaker et al., 2006). Consistent with this observation, FN is essential for early embryonic development; mice lacking FN die by embryonic day 9.5 with severe cardiovascular defects, including malformed or absent embryonic vessels and heart (George et al., 1993; Georges-Labouesse et al., 1996).

FN is a complex, alternatively spliced multidomain protein. FN domains are classified into type I (twelve domains), type II (two domains) and type III (fifteen–seventeen domains) FN repeats. In addition, FN is alternatively spliced at three regions which can be included or excluded, either completely (EIIIA, EIIIB, both type III repeats) or partially (the V region), generating up to 12 different variants in rodents and 20 in humans (Hynes, 1990; Kornblihtt et al., 1985; Kornblihtt et al., 1984a; Pankov and Yamada, 2002; Schwarzbauer et al., 1987). These splice variants are differentially expressed in development and disease, both spatially and temporally (ffrench-Constant and

Abbreviations: FN, fibronectin; EIIIA, EIIIB, extra fibronectin type III domain A or B; αSMA, alpha smooth muscle actin; PECAM, platelet/endothelial cell adhesion molecule; MEF, mouse embryo fibroblasts; ES cells, embryonic stem cells; NEM, N-ethyl maleimide; PMSF, phenylmethylsulphonyl fluoride; EDTA, ethylenediaminetetraacetic acid.

* Corresponding author. Fax: +1 617 253 8357.
E-mail address: rohynes@mit.edu (R.O. Hynes).
[1] Current address: Department of Cardiology, Weill Cornell Medical School, New York, USA.

0012-1606/$ - see front matter © 2007 Elsevier Inc. All rights reserved.
doi:10.1016/j.ydbio.2007.07.005

Hynes, 1989; ffrench-Constant et al., 1989; Peters et al., 1996; Peters and Hynes, 1996; Tan et al., 2004). The importance of some repeats is well known; for example, the 9th and 10th type III repeats as well as the V region function in cell adhesion to cell-surface integrins (Aota et al., 1991; Guan and Hynes, 1990; Hynes, 1990; Pankov and Yamada, 2002), the 13th type III repeat is important for binding to proteoglycans and for assembly of actin stress fibers (Bloom et al., 1999; Wierzbicka-Patynowski and Schwarzbauer, 2003); the functions of other repeats are not understood. While being distinct from each other in sequence, all of the FN repeats are conserved through evolution, suggesting importance of each of these repeats for the functions of FN. The alternative splicing of FN introduces another level of complexity and raises questions such as whether the inclusion or exclusion of the alternatively spliced domains alters the functions of FN and the biological consequences of their presence or absence.

Alternative splicing of EIIIA and EIIIB exons of FN is dynamically regulated *in vivo*. These splice variants are expressed at very low levels or not at all in the adult (Peters et al., 1996). However, during embryogenesis, both EIIIA and EIIIB exons become included into cellular FN (Peters and Hynes, 1996) and, in adults, these splice variants appear during pathological processes requiring growth and/or remodeling of the existing vasculature (Carnemolla et al., 1989; Glukhova et al., 1989; Peters et al., 1988; Shekhonin et al., 1990; Trachsel et al., 2007).

There is a strong correlation between the expression of EIIIA and EIIIB and the presence of vascular remodeling. During embryonic development, EIIIA and EIIIB are expressed around embryonic vessels (ffrench-Constant and Hynes, 1989; Peters and Hynes, 1996); but this expression ceases when the process of vascular development is complete (ffrench-Constant and Hynes, 1989; Peters et al., 1996). In adults, there is little or no detectable expression of EIIIA and EIIIB around quiescent vasculature in either mouse or human. However, during pathological angiogenesis, for example in the process of tumor development, these exons become included into FN. In fact, all human and murine tumors that have been examined for the presence of these splice variants show their abundant expression in the extracellular matrix surrounding tumor vessels (references in (Astrof et al., 2004; Castellani et al., 2002; Oyama et al., 1989). This correlation is so striking that it has led to the development of anti-EIIIB antibody as a tumor-targeting and a tumor-imaging reagent in mice and humans (Borsi et al., 2002; Kaspar et al., 2006; Nilsson et al., 2001).

Other pathological processes during which EIIIA and EIIIB are included in the FN are wound healing, atherosclerosis, and myocardial infarction, all of which require vascular remodeling (ffrench-Constant et al., 1989; Matter et al., 2004; Shekhonin et al., 1990). In spite of their high degree of sequence conservation among vertebrate species and the evolutionarily conserved regulation of their expression patterns, the functions of these splice variants have remained a mystery for nearly two decades since their original discovery.

A number of *in vitro* studies have claimed various, often discordant (from no effect to some) effects of inclusion of EIIIA or EIIIB exons on cell attachment, migration, proliferation, cell survival, matrix assembly, or expression of smooth muscle α actin (Chen and Culp, 1996; Guan et al., 1990; Hashimoto-Uoshima et al., 1997; Manabe et al., 1999; Serini et al., 1998; Xia and Culp, 1994). However, *in vivo*, the individual deletion of EIIIA or EIIIB has not given much insight into the possible functions of these splice variants. *EIIIA-null* or *EIIIB-null* mice are viable and fertile, and physiological angiogenesis such as embryonic vascular development and retinal angiogenesis after birth proceeded apparently normally in these mice (Astrof et al., 2004; Fukuda et al., 2002; Muro et al., 2003; Tan et al., 2004). Tumor growth and angiogenesis examined in the transgenic Rip-Tag tumor model were not significantly affected by the absence of either of the splice variants. Furthermore, contrary to expectations, the development of αSMA-positive cells was not affected (Astrof et al., 2004). However the absence of EIIIA was mildly protective in an atherosclerosis model (Tan et al., 2004). In one study, a delay in cutaneous wound healing in *EIIIA-null* mice was noted (Muro et al., 2003), but this effect was not replicated in another study (Tan et al., 2004). Interestingly, a possible effect of EIIIB on FN matrix assembly and proliferation was observed in *EIIIB-null* MEFs *in vitro* and recombinant EIIIB-positive FN incorporated somewhat more efficiently into ECM (Fukuda et al., 2002; Guan et al., 1990), suggesting a possible role for EIIIB in FN matrix assembly.

Since the EIIIA and EIIIB splice variants are highly conserved in sequence and expression pattern among species, we reasoned that simultaneous deletion of both of these exons might allow us to understand their function(s). Indeed, the absence of both EIIIA and EIIIB was embryonic lethal in the majority of embryos leading to severe cardiovascular defects. Here we report the phenotypes of the *EIIIA /EIIIB-double-null* embryos and the possible functions of EIIIA and EIIIB in vascular development.

Materials and methods

Generation of EIIIA and EIIIB double-null mice

EIIIB-null ES cells were generated from *EIIIB-null* mice (Fukuda et al., 2002) by isolating *EIIIB-null* zygotes. Zygotes were cultured in KSOM medium (Chemicon, Temecula, CA) for 3 days until blastocyst stage and then plated on a monolayer of mouse embryo fibroblasts (MEFs) in ES cell medium containing 1000 U/ml LIF (Chemicon) and 50 μM MEK inhibitor PD98059 (Cell Signalling Technology, Danvers, MA) as described (Nagy et al., 2003). Following 4 days of incubation, ES cell colonies were picked, trypsinized and plated on a monolayer of MEFs. Two independent clones of *EIIIB-null* ES cells were isolated and tested for germline transmission. One of the clones, B8, was selected for further targeting to generate the *EIIIA-null* allele. The *EIIIA-null* allele was generated as described (Tan et al., 2004) using a targeting construct generously provided by Elizabeth George, and subsequent transfection of the targeted ES cells with Cre recombinase-encoding plasmid, pMC-Cre (Gu et al., 1993). Southern blots were performed using restriction enzymes *Eco*RI, *Hin*dIII, and *Bam*HI and probe 2 (Tan et al., 2004) as well as restriction enzyme AvrII with probes 2 and sub44 (Fig. 2). Correctly targeted ES cell clones were injected into blastocysts derived from FVB/NJ mice and chimeric mice were mated with C57BL6/J wild-type mice. The progeny were genotyped using primers 5′-GTA CGT AAC CAA TGC TCG GT-3′ (primer 4) and 5′-CAC AGA CTA TTC CAT CCT AGA GAT AG -3′ (primer 5) to detect *EIIIA-null* (1233 bp) and wild-type (2092 bp) alleles and 5′-GCA CAC TTT GGA GGC CTG TCT TAG-3′ (primer 1), 5′-GAA AGC AAG CCA TGG GGG GCC TGG CC - 3′ (primer 2), 5′-CCT GGC CTG GAG TAC

AAC GTC AGT G-3′ (primer 3), to detect *EIIIB-null* (818 bp) and wild-type (616 bp; 2099 bp wild-type band was not detected under the PCR conditions used) alleles. Genomic PCR primers described previously (Fukuda et al., 2002; Tan et al., 2004) were also used to genotype *EIIIA-null* and *EIIIB-null* alleles. The PCR results were confirmed by Southern blot using AvrII restriction enzyme and probe 2 (see Fig. 2C).

Quantification of FN message and protein levels

RT-PCR

RNA from e9.5 embryos was isolated using Trizol (Invitrogen, Carlsbad, CA) according to the manufacturer's instructions. RNA was treated with RNase-free DNase, repurified and used for reverse transcription. The presence or absence of EIIIA or EIIIB exons in FN mRNA was detected as described (Astrof et al., 2004). To quantify FN mRNA levels, quantitative real-time PCR was performed using primers 5′-CCT CTC TGG AAG AAG TGG TCC-3′ and 5′-GAC GTT GTA CTC CAG GCC AG-3′ lying within the 7b (III7b) exon, primers 5′-CTC CCA CGG ATC TGC GAT TC-3′ and 5′-GGT TGG TCA GCT CGA TGG AC-3′ lying within the III8a exon and primers 5′-GTT CAG TCA GGT GAC ACC CAC-3′ and 5′-CCT GTC TTC TCT TTC GGG TTC-3′ lying within the III12a exon. RNA levels of mouse GAPDH served as controls. Incorporation of SYBR green into double-stranded PCR products was monitored using Biorad iCycler.

Western blotting

Wild-type, heterozygous and null embryos were isolated at e9.5 or e14.5. Trunks of e9.5 and heads of e14.5 embryos were lysed as described (Senger et al., 1983). Briefly, frozen embryos were resuspended in 500 μl of SDS lysis buffer using 27-gauge needle. The lysis buffer contained 0.1 M Tris–HCl pH 8.0, 0.2% SDS, protease inhibitors (one complete mini tablet (Roche, Basel, Switzerland) per 7 ml) and 2 mM NEM, 4 mM PMSF, 5 mM EDTA. The lysates were boiled for 10 min and 140 mM β-mercaptoethanol was then added. Lysates were used without centrifugation. 40 μl of each lysate were resolved on SDS-PAGE gel (5% resolving, 3% stacking), and the rest was stored at −80 °C. Rabbit polyclonal antibody 297.1 diluted 1:4000 was used to detect total (t) FN, goat polyclonal antibody 153.1 was used to detect EIIIA (Peters et al., 1996; Peters and Hynes, 1996) and mouse monoclonal antibody SAP.4G5, diluted 1:5000 was used to detect β-tubulin 1 (T7816, Sigma, St. Louis, MO). The staining was detected using affinity-purified donkey anti-rabbit, donkey anti-goat and donkey anti-mouse antibodies conjugated to horseradish peroxidase (Jackson Immunoresearch, West Grove, PA) diluted 1:3000 and Western Lightning kit (Perkin Elmer, Waltham, MA), and quantified using a Storm phosphorimager. Intensity of FN bands was normalized to that of β-tubulin bands.

Metabolic labeling

Wild-type, heterozygous and null MEFs were isolated from e14.5 embryos as described (Nagy et al., 2003). 5×10^5 cells were plated on 60-mm dishes for 24× h and labeled using ^{35}S-Methionine/Cysteine (NEN, Waltham, MA) as described (Senger et al., 1983). Briefly, cells were incubated with 200 μCi in 1 ml of medium for 2 h, supernatants were collected at 60, 80, 100 and 120 min, and resolved using 5% SDS-PAGE. To assay incorporation of FN into the cell matrix, cells were labeled for 2 h, washed, and incubated in label-free medium for 24 h. Cells were then lysed and FN was immunoprecipitated using 297.1 antibody and protein G agarose.

Immunohistochemistry and immunofluorescence

Embryos were isolated at e9.5 or e10.5, fixed with 3.75% formalin at 4 °C overnight and dehydrated through a methanol series (25%, 50%, 75%). They were then incubated with 6% H_2O_2 in methanol for 4 h, re-hydrated through the methanol series and used for whole-mount staining with anti-Pecam 1 antibody (Pharmingen, Rockville, MD). Embryos were first incubated with blocking solution (PBS, 0.1% Triton-X-100 and 10% goat serum) at 4 °C overnight, then with the anti-Pecam 1, diluted 1:100 in the blocking solution, also 4 °C overnight. Embryos were then washed with PBS containing 0.1% Triton-X-100 overnight and incubated with affinity-purified donkey anti-rat secondary antibody conjugated to horseradish peroxidase (Jackson Immunoresearch) at 4 °C overnight. After washing, the embryos were developed using DAB kit (Vector, Burlingame, CA). Embryos were then embedded into histogel (VWR, West Chester, PA), fixed with 3.75% formalin at 4 °C overnight and processed for histology into paraffin blocks. To stain for αSMA, sections were boiled in 10 mM citric acid pH 6.0 for 10 min, incubated with blocking solution containing PBS, 0.05% Tween-20 and 10% donkey serum and then with alkaline-phosphatase-conjugated antibody to αSMA (A5691, Sigma) in blocking solution. After overnight incubation at 25 °C, sections were washed and stained using NBT/BCIP solution (Roche). For detection of EIIIA, EIIIB and tFN, embryos were fixed in Zn fixative (BD Pharmingen) for 48 h at room temperature, processed for paraffin embedding and sectioned. Sections were stained using 297.1 antibody to tFN (1:1000), purified rabbit polyclonal antibody 264.1 diluted to 25 ng/ml to detect EIIIB exon, and purified goat polyclonal antibody 153.1 diluted to 140 ng/ml to detect EIIIA exon (Astrof et al., 2004). PBS containing 0.05% Tween-20 and 3% chicken ovalbumin were used as blocking solution and diluent. Staining was developed using secondary antibodies conjugated to horseradish peroxidase (described above) diluted 1:200 and DAB kit. Placentae were fixed in 3.75% formalin at 4 °C overnight, processed for paraffin embedding and sectioned. Sections were either stained with hematoxylin and eosin or with rabbit polyclonal anti-laminin-1 antibody (L9393, Sigma) diluted 1:100 followed by affinity-purified donkey anti-rabbit antibody conjugated to alkaline phosphatase (Jackson Immunoresearch) and developed using NBT/BCIP. All sections were counter-stained with methyl green and observed using an Axiophot microscope. Immunofluorescence studies to detect tFN, EIIIA and EIIIB splice variants were performed as described (Peters and Hynes, 1996).

Results

Expression of EIIIA and EIIIB splice variants during embryonic development

The expression patterns of EIIIA and EIIIB splice variants have been extensively studied previously (ffrench-Constant and Hynes, 1989; Peters et al., 1996; Peters and Hynes, 1996), however, we re-examined embryonic expression of these splice variants in selected embryonic tissues at e10.5, using limiting amounts of antibodies to detect any possible differential expression. To our surprise, not all embryonic and extra-embryonic vessels stained well with antibodies to tFN, EIIIA or EIIIB. In placental labyrinth, embryonic vessels located closer to the edge but not those located closer to the giant-cell trophoblast layer expressed FNs; maternal vessels did not detectably express FNs within the labyrinth (Figs. 1A–D). Interestingly, within the e10.5 embryo, FN and its splice variants were highly enriched around dorsal aortae and pharyngeal arch arteries but were expressed either at very low levels or not at all around anterior cardinal veins (Figs. 1E–H). Finally, in accord with previous studies (ffrench-Constant and Hynes, 1989; Peters and Hynes, 1996), we found expression of EIIIA and EIIIB around endocardial and cushion cells of the heart (Figs. 1I–K). This pattern of expression suggested that EIIIA and EIIIB splice variants might be important for vascularization of placenta, the development of dorsal aortae and cardiac cushions. To examine the role of EIIIA and EIIIB splice variants in embryonic cardiovascular development, we deleted both EIIIA and EIIIB exons from the *FN* locus.

Generation of EIIIA and EIIIB double-null animals

EIIIA and EIIIB exons of FN are separated by about 10 kb of sequence in the mouse genome, thus precluding the possibility of obtaining *EIIIA/EIIIB double-null* mice through mating of

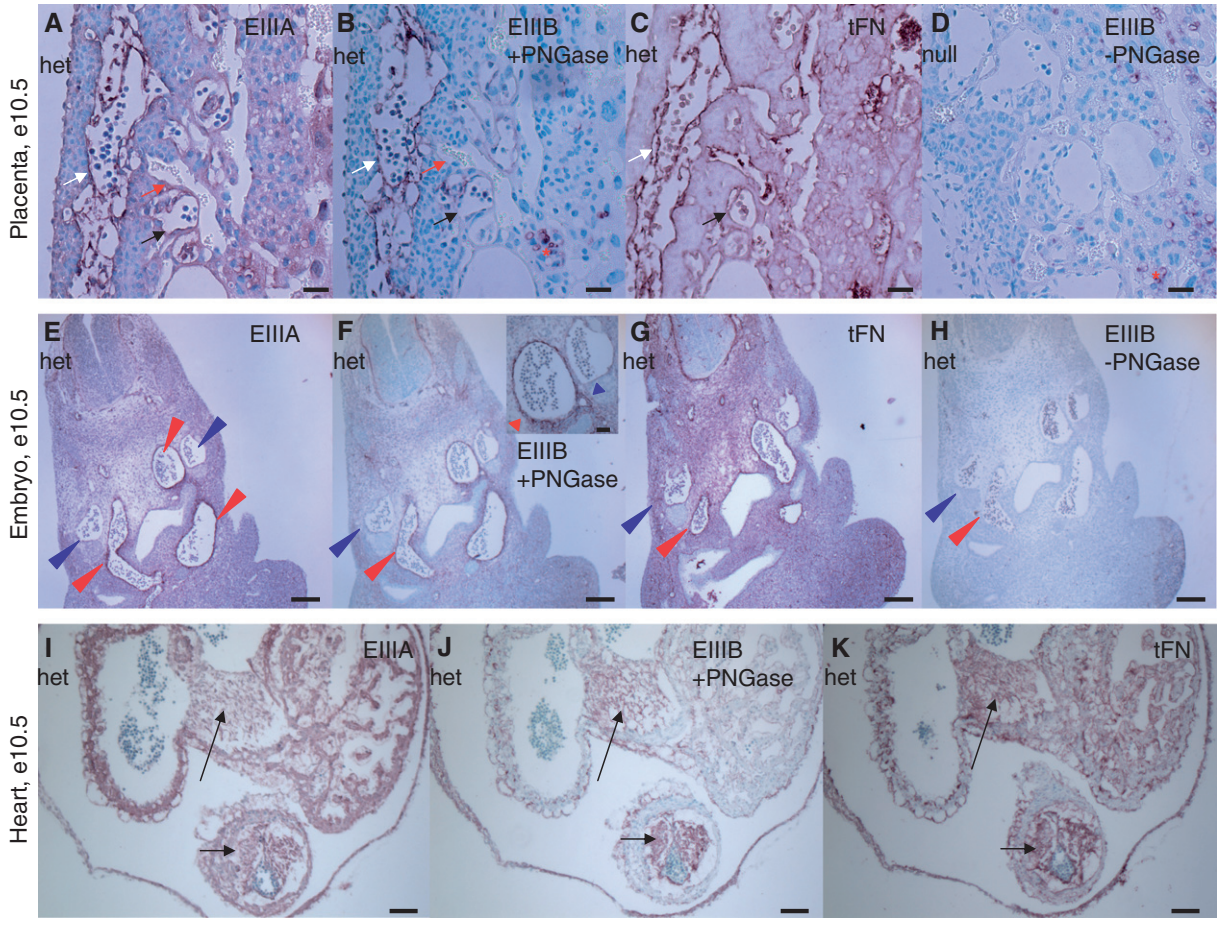

Fig. 1. Expression of EIIIA and EIIIB splice variants of fibronectin during embryonic development. (A–D) Placenta. EIIIA (A), EIIIB (B) and tFN (C) proteins are expressed around embryonic but not maternal blood vessels. (D) *EIIIA /EIIIB-double-null* placenta stained for EIIIB. White arrows point to embryonic blood vessels. Red arrows point to maternal blood vessels. Black arrows point to embryonic vessels lacking FN staining. Red asterisks mark non-specific staining (both EIIIB and PNGase-independent background staining (Peters et al., 1996)). Scale bars are 30 μm. (E–H) Embryo. tFN as well as EIIIA and EIIIB splice variants are enriched around arteries but not around veins. Red arrowheads point to arterial vessels and blue arrowheads point to anterior cardinal veins. (E) EIIIA, (F) EIIIB, (G) tFN, (H) Control—Staining for $EIIIB^{+}$-FN without PNGase treatment. Scale bars are 130 μm. (I–K) Heart. EIIIA (I), EIIIB (J) and tFN (K) are expressed in cushions (arrows) and endocardium of the heart. Scale bars are 65 μm.

EIIIA-null and *EIIIB-null* animals. To obtain the double-null mice, we isolated *EIIIB-null* male ES cells of a mixed 129P2/C57BL6/J background from *EIIIB-null* zygotes and used the targeting construct described previously for the generation of the *EIIIA-null* allele (Tan et al., 2004) to delete the EIIIA sequence in these cells. Following sequence-specific recombination, the floxed *EIIIA* allele is inserted such that the loxP sites in the *EIIIA* and *EIIIB* loci point toward each other, suggesting that treatment with Cre recombinase might result in the inversion of the region. Fig. 2A shows the wild-type and the *EIIIA-null* genomic loci, containing loxP sites in place of EIIIA and EIIIB exons, in correct and in inverted orientations. We performed five Southern blot experiments using four different restriction enzymes and two different probes to show that the *EIIIA* locus is targeted correctly (Figs. 2B (a–e)) and that the region between the EIIIA and EIIIB exons is positioned in

Fig. 2. Generation of the *EIIIA/EIIIB-double-null* allele. (A) Generation of the $EIIIA^{-}EIIIB^{-}$ allele. Top panel represents wild-type locus. A=*Avr*II, B=*Bam*HI, H=*Hin*dIII, R=*Eco*RI. Arrowheads designate PCR primers used for genotyping. Middle panel represents the correctly targeted $EIIIA^{-}EIIIB^{-}$ allele. Bottom panel shows the possible inverted allele. (B) Southern blots. Marker and band sizes are in kilobases (kb). Blots in all panels except panel c were performed with probe 2; in panel c, probe 44sub was used. (a) *Eco*RI digestion. B8 are *EIIIB-null* ES cells with the wild-type $EIIIA^{+}$ allele, lane numbers are names of targeted ES cell clones. The 0.86 kb band corresponds with the EIIIA deletion. (b) *Bam*HI digestion. The 1.9 kb band corresponds with the EIIIA deletion. (c and d) AvrII digests. The 2.9-kb fragment in panel d corresponds with the EIIIA deletion. $EIIIA^{-/-}$ and $EIIIA^{+/-}$ cells were used as controls. (e) *Hin*dIII digest. The 3 kb band corresponds with the EIIIA deletion. Arrowheads in panels c–e point to where bands corresponding with the possible inverted allele would have been located. (C) Genomic PCR for *EIIIB* allele (a) and a Southern blot (b, AvrII, probe 2) for EIIIA allele from a litter of nine e9.5 embryos derived from $EIIIA^{-}EIIIB^{-}/EIIIA^{+}EIIIB^{+}$ intercross. Asterisks denote double-null embryos. (D) (a) Genomic PCR to detect $EIIIA^{+}$, $EIIIB^{+}$, $EIIIA^{-}$, and $EIIIB^{-}$ alleles, (b) RT-PCR to detect $EIIIA^{+}$, $EIIIB^{+}$, $EIIIA^{-}$, and $EIIIB^{-}$ mRNA, and (c) Western blot to detect tFN, EIIIA and β-tubulin from a litter of six e9.5 embryos derived from $EIIIA^{-}EIIIB^{-}/EIIIA^{+}EIIIB^{+}$ intercross. Asterisks denote double-null embryos. (E) (a) Time-course of FN secretion into the medium and (b) FN incorporation into the extracellular matrix of metabolically labeled wild-type, double-null and double-het MEFs.

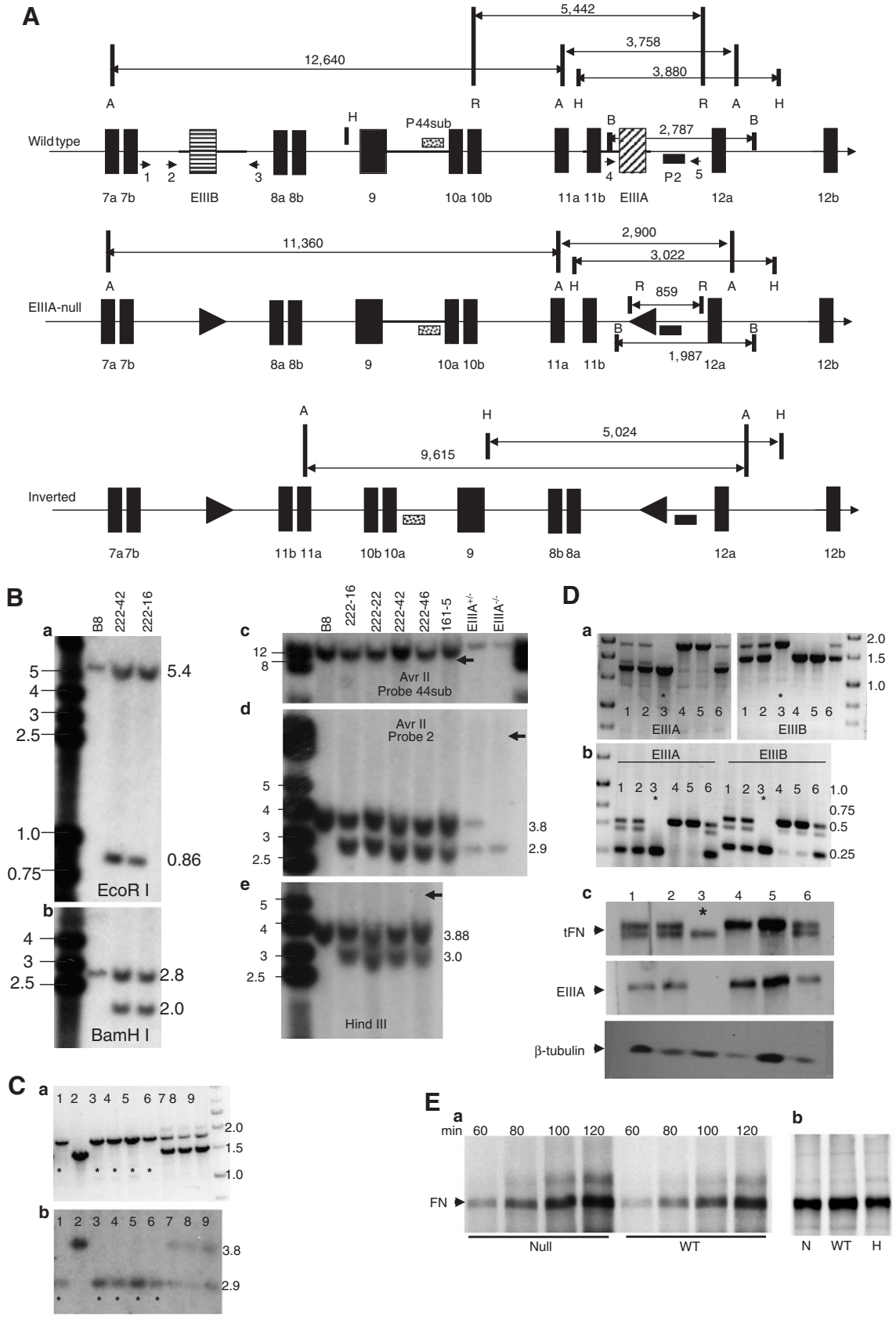
A
5,442
3,758
12,640
3,880
A
R
A H
R A H
Wild type
P44sub
2,787
1 2 3 4 P2 5
7a 7b EIIIB 8a 8b 9 10a 10b 11a 11b EIIIA 12a 12b
11,360
2,900
3,022
EIIIA-null
859
1,987
7a 7b 8a 8b 9 10a 10b 11a 11b 12a 12b
9,615
5,024
Inverted
7a 7b 11b 11a 10b 10a 9 8b 8a 12a 12b
B
B8 222-42 222-16
EcoR I
5.4
0.86
BamH I
2.8
2.0
B8 222-16 222-22 222-42 222-46 161-5 EIIIA+/- EIIIA-/-
Avr II Probe 44sub
Avr II Probe 2
3.8
2.9
Hind III
3.88
3.0
D
EIIIA
EIIIB
tFN
β-tubulin
C
E
min 60 80 100 120 60 80 100 120
FN
Null
WT
N WT H

the correct orientation with respect to *FN* (Figs. 2B (c–e)). The targeted *EIIIA*$^{-}$*EIIIB*$^{-}$/*EIIIA*$^{+}$*EIIIB*$^{-}$ ES cells were then injected into FVB/NJ wild-type blastocysts and the resulting chimeric mice were mated to wild-type C57BL6/J females. We verified the transmission of the *EIIIA*$^{-}$*EIIIB*$^{-}$ allele using Southern blotting (data not shown) and intercrossed *EIIIA*$^{-}$*EIIIB*$^{-}$/*EIIIA*$^{-}$*EIIIB*$^{+}$ mice to obtain e9.5 embryos, which were then used to verify the absence of EIIIA and EIIIB sequences in the *FN* DNA, mRNA and protein of the double-null embryos (Figs. 2C, D and 3). Our data indicate that, indeed, the double-null embryos lacked both EIIIA and EIIIB exons (Figs. 2C and 3) and that the deletion of both of these exons did not compromise the expression of FN mRNA (Fig. 2D) and protein (Figs. 2C and 3), nor the deposition of FN into the matrix (Fig. 2E, Fig. S1 and Table S1).

Interbreeding of *EIIIA*$^{-}$*EIIIB*$^{-}$/*EIIIA*$^{+}$*EIIIB*$^{+}$ mice (mixed C57BL6/J and 129P2 background) produced only 18% of the expected number of double-null adults (Table 1), suggesting that the absence of both EIIIA and EIIIB is embryonic lethal with about 80% penetrance. Indeed, 50% of e9.5 and 80% of e10.5 double-null embryos showed severe cardiovascular defects (Fig. 4), and were absorbed by e11.0 (Table 1 and data not shown). Interestingly, the ability to survive in the absence of EIIIA and EIIIB had a statistically significant genetic background component (Table 1). Intercrosses of double-heterozygous mice, backcrossed six times to 129S4 strain, did not produce any live progeny (fifty seven live mice were examined, representing nine litters), while about 50% of the expected number of the double-null mice were born from *EIIIA*$^{-}$*EIIIB*$^{-}$/*EIIIA*$^{+}$*EIIIB*$^{+}$ mice backcrossed six times to C57BL6/J strain (thirty three live mice were examined, representing eight litters). The partial viability of *EIIIA/EIIIB-double null* mice bred to C57BL6/J as opposed to 129S4 background is consistent with the observation that the phenotype of *FN-null* mice is milder on C57BL6/J than on 129S4 background (George et al., 1997; Astrof et al., in press).

Table 1

Genotype			Age
Wild type	Het	Null	
88	145	12	Adult (129S4/C57BL6/J mixed)
18	39	0	Adult (129S4) [a]
10	19	4	Adult (C57BL6/J)[a]
19 (1)	44 (3)	26 (12)	e9.5(129S4/C57BL6/J mixed)
15 (1)	43 (4)	16 (13)	e10.5(129S4/C57BL6/J mixed)

Numbers in parenthesis are the numbers of abnormal embryos.
[a] These distributions are statistically different: $p=0.002$, χ^2 test.

Phenotypes of EIIIA and EIIIB double-null embryos

There was heterogeneity of phenotype among the double-null embryos in the mixed background crosses. About half of the double-null embryos of mixed genetic background showed severe cardiovascular defects by e9.5. These defects included hemorrhage within the embryo (83% of all defective embryos) and anemia due to leakage of blood (Figs. 4A, B, G), shortened posterior, kinked neural tube (5% of all defective embryos) (Fig. 4A) and blistered appearance of the yolk sac (30% of all defective embryos) resulting from separation of endodermal and mesodermal layers (Figs. 4B, J, K). These defects are reminiscent of, but milder than, the defects in *FN-null* or in FN-receptor, *integrin α5-null* embryos. By e10.5 about 80% of the double-null embryos showed vascular defects (Figs. 4D, E). These defects included embryonic hemorrhage (100%), dilation of pericardial cavity (50%), and thinned outflow tract (30%) (Fig. 4D). A small number of double-null embryos (about 7%) appeared morphologically normal (compare Figs. 4E and F) but exhibited focal hemorrhage in the head (Figs. 4E, I); the yolk sac vasculature and the heart developed normally in these embryos (data not shown).

Embryonic vascular development in the double-null embryos was analyzed by detecting vessels with antibody specific for the endothelial marker Pecam-1 (Fig. 5; summarized in Table 2). At

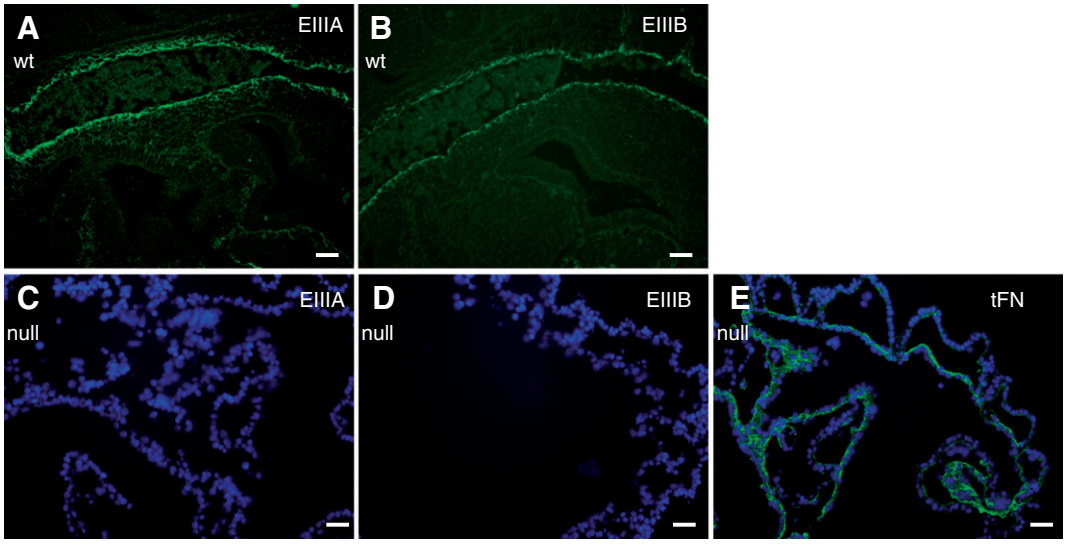

Fig. 3. *EIIIA/EIIIB-double-null* embryos express only EIIIA^{-} and EIIIB^{-} FN. (A) Sagittal sections through e9.5 embryos show expression of EIIIA^{+} and (B) EIIIB^{+} −FN in wild-type littermate control embryos. The vessel stained is dorsal aorta. (C–E) Yolk sacs of e 9.5 *EIIIA/EIIIB-double-null* embryos show lack of EIIIA (C) and EIIIB (D) expression, whereas FN (E, green) is expressed. DAPI was used to stain nuclei. Scale bars are 30 μm.

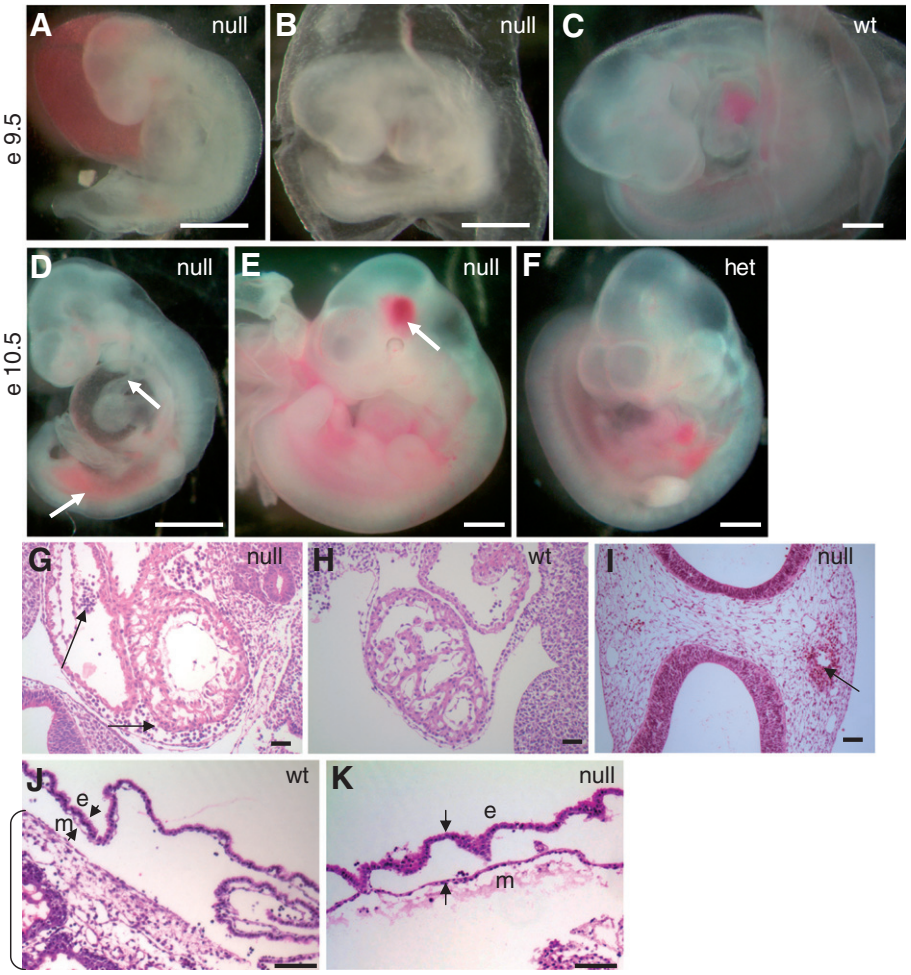

Fig. 4. Phenotypes of *EIIIA/EIIIB-double-null* embryos. (A–C) Representative double-null (A, B) and wild-type (C) embryos at day e9.5 of development are shown. Note hemorrhage, truncated posterior and a kinked neural tube in panel A, and avascular and blistered yolk sac in panel B. (D–F) Representative double-null (D, E) and wild-type (F) embryos at e10.5 are shown. Note shortened and hemorrhagic posterior and a thinned outflow tract (arrows) in panel D and a localized head hemorrhage (arrow) in panel E. Scale bars are 1 mm. (G–I) Sagittal sections through embryonic hearts at e9.5 (G, H) and a transverse section through an e10.5 embryonic head (I). Arrows in panel G point to blood in pericardial cavity as well as in the space between endocardial and muscle layers; arrows in panel I points to hemorrhage in the head. Scale bars are 30 μm. (J, K) Sections through wild-type and double-null yolk sacs. Arrowheads mark mesodermal (m) and endodermal (e) layers. Note the separation of these layers in panel K. Bracket marks placenta in panel J.

e9.5, double-heterozygous embryos (Fig. 5A) and some morphologically normal double-null embryos (Fig. 5B) had correctly patterned vasculature with large vessels and a finely patterned vascular plexus in the head and body. In contrast, in severely affected double-null embryos (Fig. 5C) and even in some morphologically normal e9.5 double-nulls (Fig. 5D), there were few and dysmorphic large vessels in the head, and small vessels in the head and body appeared syncytial with endothelial cells forming sheets instead of tubes (Figs. 5C, D, I, J). Interestingly, we observed two kinds of vascular defects in morphologically normal double-nulls. Some of them presented with a syncytial head vasculature (Fig. 5D), these embryos would presumably be dying by e10.5; others developed a normal vascular plexus of small vessels but abnormal patterning of the large head veins, where vessels appeared blunt-ended and discontinuous (Fig. 5E).

Vascular defects in the double-null embryos at e10.5 could also be divided into two groups—the most severely affected embryos had syncytial vasculature with endothelial cells forming sheets instead of tubes (Fig. 5G) and less severely affected, morphologically normal double-null embryos, with abnormally patterned, blunt-ended and constricted head veins (Fig. 5H). It is plausible that one of these constricted vessels could rupture leading to focal hemorrhage in the head.

Extraembryonic vascular defects

Most but not all morphologically abnormal double-null embryos exhibited defects in the development of yolk sac and placental vasculature. Embryos with blistered yolk sacs had unremodeled and dilated yolk sac vessels and a general lack or degeneration of large vessels (Figs. 6A–D and data not shown). About 90% of embryos showing severe intra-embryonic vascular defects also had defective yolk sac vasculature, suggesting that EIIIA and EIIIB splice variants function in embryos and yolk sacs to remodel the initial uniform vascular plexus into a more mature pattern with large and small vessels.

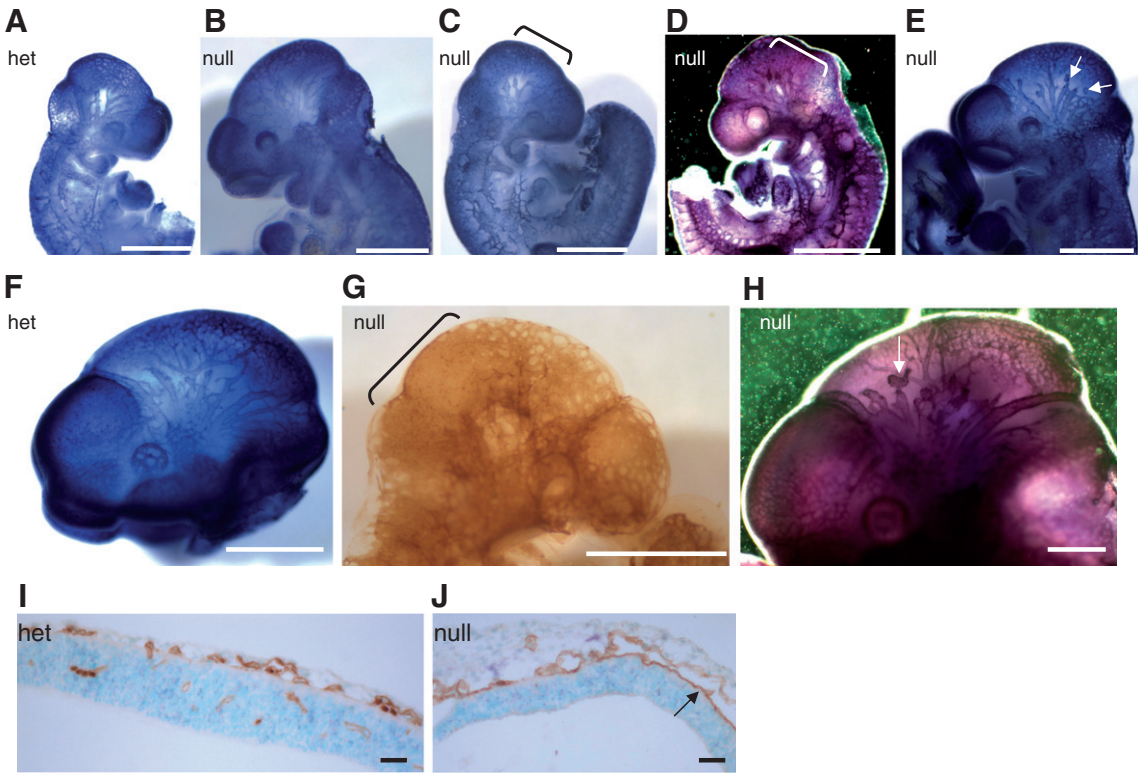

Fig. 5. Head vasculature in double-null embryos at e9.5 and e10.5. (A–E) Pecam-1 staining of e9.5 heads. Note a regular pattern of small and large blood vessels in a heterozygous (A) and in a grossly normal double-null embryo (B), compared with a syncytial appearance of small head vessels in a morphologically defective (C) and a grossly normal (D) double-null embryo. Note blunt-ended and interrupted vessels in another grossly normal double-null embryo (E). (F–H) Pecam-1 staining of e10.5 heads. Note a regular pattern of small and large vessels in a heterozygous (F) embryo as opposed to syncytial appearance of small vessels and the scarcity of large vessels in a morphologically abnormal double-null embryo (G), as well as short, blunt-ended and interrupted head vessels in a grossly normal double-null (H). Brackets highlight syncytial endothelial sheets in panels C, D and G and arrows point to blunt-ended vessels in panels E and H. Scale bars are 1 mm in all except panel H, where scale bar is 240 μm. (I–J) Transverse sections through heads of a heterozygous (I) and a double-null (J) embryo at e10.5 show the presence of small vessels in the head and vessel invasion into the neural fold in the heterozygote (I). In the double-null (J) the vessels appear dilated, resulting from two sheets of endothelial cells touching each other in some places. Also note the lack of vascular invasion into the neural fold in the double-null (J). Scale bars are 65 μm.

Placental vascularization was also defective in some (~50%) of the abnormal double-null embryos (Figs. 6E–H). Starting at e8.5, embryonic vessels invade placenta and by e10.5 form elaborate finger-like projections in the placental labyrinth (Figs. 6E, G). However, in about 50% of the double-null embryos, placental vascularization following the invasion with embryonic vessels was much less extensive (Figs. 6F, H). While vessels did enter the labyrinth layer initially in these embryos, they failed to form extensive projections and branches, suggesting that EIIIA and EIIIB splice variants are important for vascularization of this initially avascular placental layer. Since only about half of the e9.5 and e10.5 abnormal embryos had defects in placental vascularization, aberrant placental development was not the cause or the consequence of embryonic vascular defects, suggesting independent roles for EIIIA and EIIIB in both embryonic and placental vascular development. Similarly, defective yolk sac vasculature was not a cause or a consequence of defective placental angiogenesis, suggesting independent roles for EIIIA and EIIIB splice variants in both yolk sac and placental vascularization. Thus, these different developmental

Table 2

	Appearance of head vessels [a]					
	e9.5			e10.5		
	Normal	Syncytial [b]	Blunt [c]	Normal	Syncytial	Blunt
Grossly abnormal nulls	0	2	0	0	5 [d]	1
Grossly normal nulls	2	3	2	2	0	2
Grossly normal hets	10	1	0	5	0	0

[a] Detected by anti-Pecam-1 antibody staining.
[b] Syncytial refers to the appearance of small vascular plexus in the head.
[c] Blunt refers to the appearance of large head veins.
[d] In addition to these five, two other embryos had unremodeled head vasculature with dilated small vessels and very few large vessels in the head.

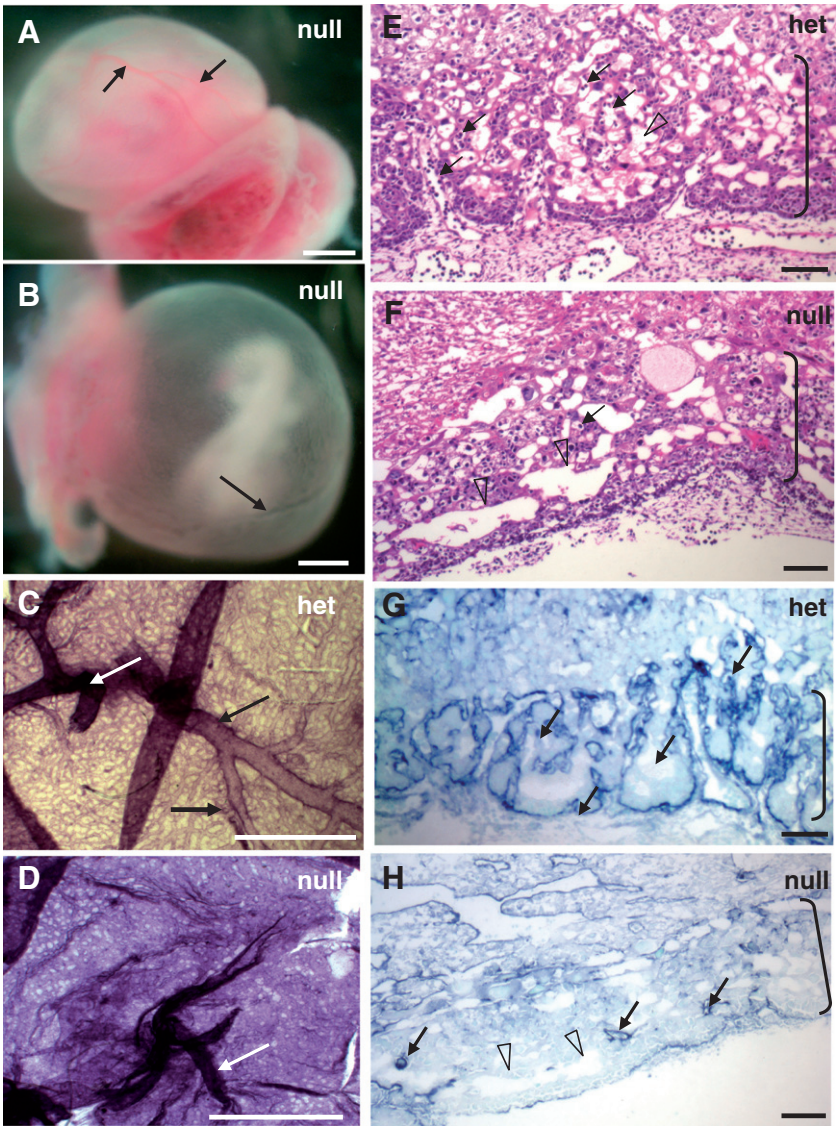

Fig. 6. Extraembryonic vascular defects in *EIIIA/EIIIB-double-null* embryos. (A–D) Yolk sacs. (A, B) *EIIIA/EIIIB-double-null* yolk sacs showing normal (A) and defective (B) vasculature. Yolk sac in panel A has large (arrows) and small blood vessels while the one in panel B has only one large vessel (arrow) and abnormally patterned small vessels. (C, D) A heterozygous and a double-null yolk sac stained with antibody to Pecam-1. White arrows point to vitelline vessels and black arrows point to large yolk sac blood vessels. Notice the size and the regular pattern of yolk sac vessels in panel C, and syncytial appearance of vasculature and absence of large blood vessels in panel D. Scale bars are 1 mm. (E–H) Placental labyrinths (brackets) in heterozygous (E and G) and double-null (F and H) embryos. Note extensive embryonic vasculature permeating the labyrinthine layer in panel E and the scarcity of embryonic blood vessels in panel F. Filled arrows point to embryonic and open arrowheads to maternal vessels. (G, H) Vascular pattern in the labyrinth layer is revealed with an antibody to laminin1. Note abundant finger-like vascular projections in heterozygous (G) but not double-null (H) placenta. Scale bars are 65 μm.

defects in different vascular beds can be uncoupled and appear to be independent consequences of the lack of EIIIA and EIIIB splice variants.

Heart defects in the EIIIA/EIIIB double-null embryos

Most of the affected double-null embryos had gross morphological heart defects such as edema and thinned or dilated outflow tracts (Figs. 4D, 7A). Some embryos (three out of six morphologically abnormal e10.5 double-nulls analyzed) had defects in cardiac cushion formation (Figs. 7A, Ba and Fig. S2). One of the embryos contained multilayered endothelium in the outflow tract with no evidence of cushion cell differentiation (Fig. 7Ba), another had multiple layers of endothelium in the atrio-ventricular cushions (not shown), while in the third double-null embryo, cushion cells did develop, but were cuboidal in shape and did not express phosphorylated SMAD2 (Fig. S2), suggesting a role for EIIIA and EIIIB splice variants in transformation of endocardial cells into cushion cells.

Vascular smooth muscle cell development in the double-null embryos

Earlier studies had suggested a role for EIIIA in induction of αSMA (Serini et al., 1998). However, our previous studies indicated that, individually, the absence of either EIIIA or EIIIB

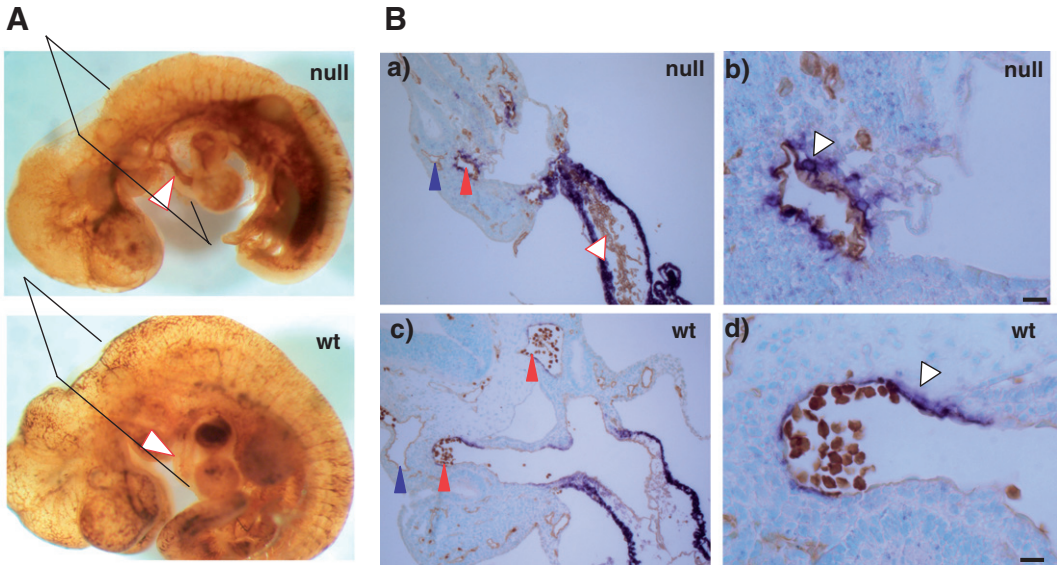

Fig. 7. Defects in heart cushion formation and in association of αSMA cells with dorsal aortae of e10.5 embryos. (A) Whole mount Pecam-1 stain revealing blood vessel pattern. Arrowheads point to outflow tracts in double-null and wild-type embryos. Notice a thin outflow tract as well as abundant Pecam-1 reactivity within the outflow tract of the double-null embryo as compared with the wild-type embryo. (B) Transverse sections through embryonic hearts. Notice multilayering of endothelial cells in (a) compared with (c). Scale bars are 130 μm. (b and d) αSMA cells are closely associated with dorsal aorta in the wild-type embryos while in the double-null embryo, the αSMA cells are rounded and not well spread around the vessel. Scale bars are 15 μm.

did not affect expression of αSMA in tumor stroma (Astrof et al., 2004). Specific expression of FN and its splice variants around dorsal aortae in embryos suggested that these splice variants might play a role in the development of aortic vessels during embryogenesis. The most notable difference between dorsal aortae and anterior cardinal veins in e9.5 and e10.5 embryos is the presence of vascular smooth muscle cells expressing αSMA specifically around dorsal aortae but not around anterior cardinal veins (Fig. 7; (Li et al., 2003). To examine smooth muscle cell association with the aortae, e9.5 and e10.5 embryos were stained using both anti-Pecam 1 and anti-αSMA antibodies, and the number, association, and morphology of αSMA-positive cells were assessed. Enumeration of αSMA-positive cells around dorsal aortae at e9.5 indicated that there was a statistically significant difference in the number of αSMA-positive cells closely associated with dorsal aortae in *EIIIA/EIIIB-double null* embryos compared with their heterozygous littermates (Figs. 8A, B). Both morphologically normal and abnormal double-null embryos showed a decrease in the number of vascular smooth muscle cells (Fig. 8A). By e10.5 most of the dorsal aortae in morphologically abnormal double-null embryos were surrounded by αSMA-positive cells, suggesting that there is only a delay in recruitment or differentiation of these cells in the double-nulls. Interestingly, three of five double-null embryos at e10.5 contained αSMA-positive cells beyond the immediate vicinity of the vessels (Figs. 8C–E), suggesting that there is a defect in migration of αSMA-positive cells to dorsal aortae in the double-null embryos. These e10.5 double-null embryos also had defective association of αSMA-positive cells with the endothelium of dorsal aorta (Figs. 7B, a–d). Instead of being closely opposed to the endothelial lining of the vessel, the αSMA-positive cells were rounded, suggesting a defect in vascular smooth muscle cell spreading along the vessel wall. Taken together, our experiments suggest that EIIIA and EIIIB splice variants function in recruitment, differentiation and associations of aortic αSMA cells to vessels in vivo.

Discussion

The alternative splicing of EIIIA and EIIIB was discovered about 20 years ago (Kornblihtt et al., 1984b; Schwarzbauer et al., 1987) and a myriad of studies that followed attempted to address the functions of EIIIA and EIIIB splice variants in cell culture and in vivo. However, this turned out to be a difficult problem largely because FN is a complex multidomain protein. It is difficult to produce full-length FN in a recombinant form and it is hard to deplete cells or media completely of FN, hampering reconstitution studies. Unexpectedly, mice carrying individual deletions of EIIIB or EIIIA exons were viable and fertile (Fukuda et al., 2002; Muro et al., 2003; Tan et al., 2004,), and did not provide insight into why the sequences and patterns of expression of EIIIA and EIIIB are so highly evolutionarily conserved. It is possible that EIIIA and EIIIB are overlapping in function. However, the fact that their sequences are only about 30% identical to each other in a given species argues to some extent against this model. Alternatively, while EIIIA and EIIIB may be important in the same biological process (e.g. blood vessel development), their functions could differ, but the presence of one splice variant is sufficient to support life in the artificial environment of a mouse cage. Lastly, the phenotypes of gene deletions often vary depending on genetic background, and it is possible that unknown genetic factors allowed the survival and function of *EIIIA-null* or *EIIIB-null* mice, both of which have been backcrossed to C57BL6/J genetic background.

Analysis of genomes from different phyla have suggested that FN is unique to vertebrates (Whittaker et al., 2006). The

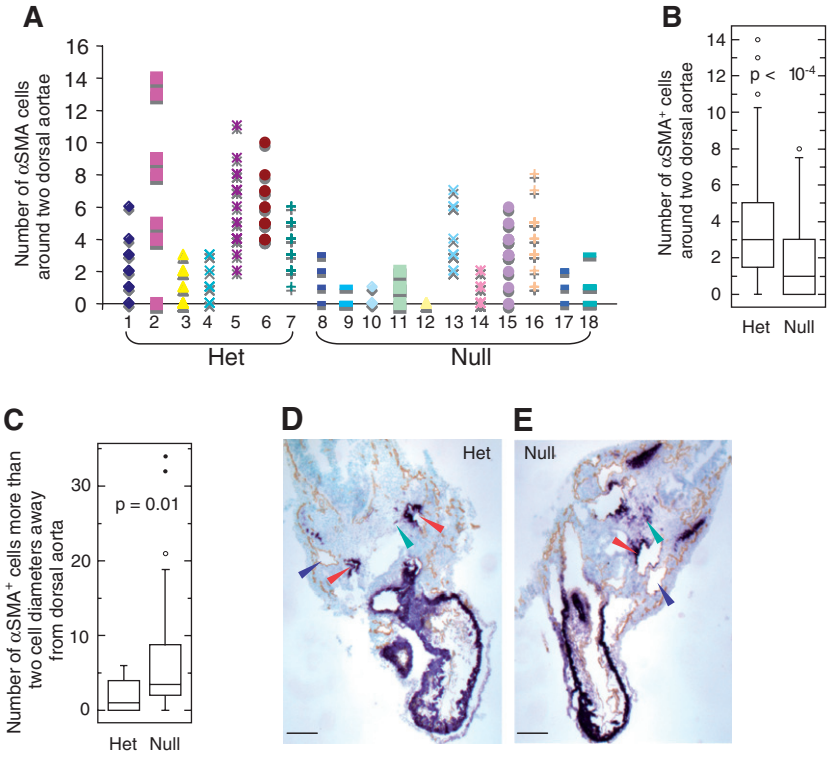

Fig. 8. Quantification of αSMA cells around dorsal aortae at e9.5 and e10.5. αSMA cells around each of the two dorsal aortae were enumerated. (A) 97 serial sections from seven heterozygous embryos representing four different litters and 126 serial sections from eleven double-null embryos representing five different litters were examined. The numbers of αSMA cells per section around the two dorsal aortae are plotted. Individual embryos are presented along the abscissa. Embryo number 10 was anemic. (B) Summary of the results in panel A presented as a box plot (the box contains the middle 50% of the data, the horizontal line within the box is the median, points outside of the whiskers (10–90% of data) are outliers). (C) Delay in recruitment of αSMA cells to dorsal aortae in embryos at e10.5 dpc. Three out of five closely examined, morphologically defective double-null embryos representing three different litters had a defect in recruitment of αSMA^+ cells to dorsal aortae. (D, E) Transverse sections through a heterozygous and a double-null embryo stained with antibodies to Pecam-1 and αSMA show excess of αSMA^+ cells outside of the immediate proximity of the dorsal aortae. Blue and red arrowheads point to veins and arteries respectively, green arrowhead points to αSMA^+ cells. Scale bars are 130 μm.

expression pattern of FN together with the severe vascular abnormalities in FN-null embryos suggested that FN functions in blood vessel development and may have evolved for that purpose. The alternatively spliced forms of FN containing EIIIA and EIIIB are also expressed around developing vasculature suggesting that they too may function in some aspect of vessel development. Indeed, we found that the absence of both EIIIA and EIIIB exons from FN message resulted in embryonic lethal cardiovascular defects.

The absence of EIIIA and EIIIB gives rise to pleiotropic vascular defects ranging from severe to mild malformations and some progeny survive. We noticed that about 20% of double-null mice were viable and fertile on a mixed 129P2/C57BL6/J background, while on a relatively pure C57BL6/J (six generations of backcrossing) about 50% survived to adulthood, appeared normal and were fertile (unpublished data). In contrast, no adult double-null mice have been observed in 129S4 strain (backcrossed for six generations). Thus the pleiotropic nature of the cardiovascular defects in the EIIIA/EIIIB double-null mice could in part be explained by segregating genetic factors in the mixed 129P2/C57BL6/J population. We have previously reported that the embryonic-lethal phenotype of FN-null embryos is more severe on a 129S4 than a C57BL/6 background (George et al., 1997) and we have mapped a strain-specific genetic modifier affecting the difference (Astrof et al., in press). It is possible that the same modifier is affecting the phenotype of the EIIIB/EIIIA double-null embryos and this will need to be investigated.

Most of the defective embryos showed various forms of heart defects. The most severely affected embryos displayed heart defects by e9.5. These defects included inflated pericardial cavity, pericardial edema, degenerating linear heart tube, or dilated aortic sac (data not shown). The embryos surviving to e10.5 also had similar defects. Since EIIIA and EIIIB splice variants are expressed in endocardial cells and in cardiac cushion cells, we examined whether there is a defect in the development of cardiac cushions. Three out of the six closely examined e10.5 embryos showed cushion defects, suggesting a role for EIIIA and EIIIB in this epithelial to mesenchymal transition in the heart. It is possible that examination of cardiac malformations in a pure background (129S4 or C57BL6/J) may decrease variability in the phenotype making it more amenable to study.

Not all vascular beds were defective in EIIIA/EIIIB double null mice; for example, small vessels in the yolk sac, head and trunk were syncytial in the severely affected embryos, but endothelial tubes of dorsal aortae and intersomitic vessels formed apparently normally. This could be due to different requirements for EIIIA and EIIIB in blood vessel development

in different embryonic compartments. In addition, EIIIA and EIIIB seem to play distinct roles in vascularization of different tissues. For example, in severely affected embryos, the absence of EIIIA and EIIIB in yolk sacs and in the head resulted in defective vascular remodeling while in the placenta, the absence of EIIIA and EIIIB led to defects in angiogenesis (sprouting of the new vessels from the pre-existing ones).

Embryonic vessels in the placenta are derived from allantoic vessels, which invade the placental labyrinth following the attachment of allantois to placenta by e8.5 of development. We did not see any differences in the invasion of the labyrinth layer by embryonic vessels, neither at e8.5 nor at e9.5 (data not shown), however we observed many fewer vessel sprouts in the labyrinth of some e10.5 embryos suggesting that, in the placenta, EIIIA and EIIIB function in vessel sprouting. It is unclear why vascularization of only some placentae was affected. This could be due to genetic differences or stochastic events. In either case, embryonic vascular defects did not arise as a consequence of defective placental vascularization since only about half of the defective embryos exhibited defective placentae. In support of this conclusion, *Gcm-1* null embryos, in which placental labyrinth does not have any embryonic blood vessels, do not develop intra-embryonic vascular defects (Anson-Cartwright et al., 2000).

FN-null mutations in mice and zebrafish as well as FN-blocking experiments in frogs showed that the absence of FN affects organ assembly but not specification of precursor cells (George et al., 1993; Marsden and DeSimone, 2001; Marsden and DeSimone, 2003; Trinh and Stainier, 2004). For example, somite, notochord and heart precursors are specified but none of these assemble into proper somites, notochord or heart structures. While the molecular mechanisms of these defects are not completely clear, in both zebrafish and frogs, the absence of FN alters cell polarity leading to defects in polarized cell movements during migration of heart primordia toward the midline in fish or during convergent extension in frogs. Vascular defects in *FN-null* and *EIIIA/EIIIB-null* embryos could also be a consequence of defects in endothelial cell polarity resulting in aberrant endothelial tube formation. Small vessels do not form properly in the heads of severely affected *EIIIA/EIIIB double-null* embryos; instead of distinct vessel tubes, we observed two sheets of endothelial cells that occasionally touch each other forming dilated vessel lumens (very similar to the ones seen in severely affected yolk sacs). Studies of tube formation during the past 10 years have shown that lumen formation in epithelial or endothelial systems (and others) requires the establishment of apical (luminal) and basolateral (abluminal) polarity through the biogenesis of apical cell surfaces and exocytosis of vacuoles at the apical membrane (Lubarsky and Krasnow, 2003). It is tempting to speculate that formation of endothelial sheets instead of tubes may be due to a defect in endothelial apical–basolateral polarity in the absence of both EIIIA and EIIIB.

While aortae do form in *EIIIA/EIIIB double-null* embryos, we noticed a statistically significant difference in the numbers of αSMA^+ cells immediately surrounding each dorsal aorta. At e9.5, there were three-fold fewer αSMA^+ cells around aortae in the double-null embryos compared with their heterozygous littermates. With the exception of a few embryos that had very few aortic αSMA^+ cells, by e10.5 most of the double-null embryos contained αSMA^+ cells around their aortae suggesting that there is a delay in recruitment or differentiation of αSMA^+ cells in the double-null embryos. Whereas present experiments cannot precisely distinguish between these possibilities, we think that there is a delay in recruitment of these cells since in e10.5 embryos some αSMA^+ cells surround the dorsal aortae but a number of others are located a few cell diameters away from the actual vessel. Interestingly, αSMA^+ cells around dorsal aortae are derived from paraxial mesodermal precursors that also give rise to somites. These precursors express *Pax3* and are seen migrating toward the dorsal aortae from their paraxial locations (Esner et al., 2006). It would be interesting to examine migration of these cells in *EIIIA/EIIIB double-null* embryos.

Whatever the cellular mechanisms contributing to the vascular defects we describe, it will also be necessary to define the underlying molecular functions of the EIIIA and EIIIB segments. As discussed earlier, this has proven to be difficult in the past but future studies will be given impetus by the evidence for important in vivo functions of these segments. It has been reported that the EIIIA segment can bind to integrins $\alpha4\beta1$ and $\alpha9\beta1$ (Liao et al., 2002) and to the Toll-4 receptor (Okamura et al., 2001), although the functional implications of these bindings have not been elucidated. Fibronectin has also been reported to bind several growth factors involved in angiogenesis; VEGF (Wijelath et al., 2002) and HGF (Rahman et al., 2005). The potential involvement of these various properties in vascular development will need to be investigated.

The existence of the alternatively spliced EIIIA and EIIIB segments of FN has been known for 20 years and the high level of conservation of their sequences and of their tightly regulated patterns of splicing has indicated that they provide some evolutionary conserved function(s). However, in vitro analyses over the past two decades have failed to reveal clear roles for these segments. Our studies demonstrate for the first time that EIIIA and EIIIB-containing splice variants of FN are crucially involved in cardiovascular development. The molecular mechanisms of their functions, as well as elucidation of the individual roles of EIIIA and EIIIB, will await further detailed in vitro and in vivo studies. The mice we report here and cells derived from them will provide valuable reagents for these investigations. The availability of mouse strains showing both embryonic defects and postnatal viability (depending on genetic background) will allow analyses of a variety of developmental, physiological and pathological situations.

Acknowledgments

We thank Elizabeth George for the EIIIA targeting construct, probes for Southern blot, pMC-Cre, a cre-expression vector, and advice on generating the EIIIA deletion; Kevin Eggan for demonstration and advice on isolation and culturing of ES cells; Adam Lacy-Hulbert and Arjan van der Flier for advice on generating the *EIIIA-null* allele as well as helpful discussion; Peimin Qi and the MIT transgenic facility for generating chimeric mice; Yueyi Zhang and Rosaria Chiang for immuno-

histochemical staining; Patrick Stern and Nathan Astrof for discussion and ideas. This research was supported by the National Heart Lung and Blood Institute, NIH (PO1-HL066105 and by the Howard Hughes Medical Institute) to ROH. S.A. was supported by postdoctoral fellowship grant PF-01-146-01-CSM from the American Cancer Society. ROH is an Investigator of the Howard Hughes Medical Institute.

Appendix A. Supplementary data

Supplementary data associated with this article can be found, in the online version, at doi:10.1016/j.ydbio.2007.07.005.

References

Anson-Cartwright, L., Dawson, K., Holmyard, D., Fisher, S.J., Lazzarini, R.A., Cross, J.C., 2000. The glial cells missing-1 protein is essential for branching morphogenesis in the chorioallantoic placenta. Nat. Genet. 25, 311–314.

Aota, S., Nagai, T., Yamada, K.M., 1991. Characterization of regions of fibronectin besides the arginine–glycine–aspartic acid sequence required for adhesive function of the cell-binding domain using site-directed mutagenesis. J. Biol. Chem. 266, 15938–15943.

Astrof, S., Crowley, D., George, E.L., Fukuda, T., Sekiguchi, K., Hanahan, D., Hynes, R.O., 2004. Direct test of potential roles of EIIIA and EIIIB alternatively spliced segments of fibronectin in physiological and tumor angiogenesis. Mol. Cell. Biol. 24, 8662–8670.

Astrof, S., Kirby, A., Lindblad-Toh, K., Daly, M.J., Hynes, R.O., in press. Heart development in fibronectin-null mice is goverened by a genetic modifier on chromosome four. Mech. Dev.

Bloom, L., Ingham, K.C., Hynes, R.O., 1999. Fibronectin regulates assembly of actin filaments and focal contacts in cultured cells via the heparin-binding site in repeat III13. Mol. Biol. Cell 10, 1521–1536.

Borsi, L., Balza, E., Bestagno, M., Castellani, P., Carnemolla, B., Biro, A., Leprini, A., Sepulveda, J., Burrone, O., Neri, D., et al., 2002. Selective targeting of tumoral vasculature: comparison of different formats of an antibody (L19) to the ED-B domain of fibronectin. Int. J. Cancer 102, 75–85.

Carnemolla, B., Balza, E., Siri, A., Zardi, L., Nicotra, M.R., Bigotti, A., Natali, P.G., 1989. A tumor-associated fibronectin isoform generated by alternative splicing of messenger RNA precursors. J. Cell Biol. 108, 1139–1148.

Castellani, P., Borsi, L., Carnemolla, B., Biro, A., Dorcaratto, A., Viale, G.L., Neri, D., Zardi, L., 2002. Differentiation between high- and low-grade astrocytoma using a human recombinant antibody to the extra domain-B of fibronectin. Am. J. Pathol. 161, 1695–1700.

Chen, W., Culp, L.A., 1996. Adhesion mediated by fibronectin's alternatively spliced EDb (EIIIB) and its neighboring type III repeats. Exp. Cell Res. 223, 9–19.

Esner, M., Meilhac, S.M., Relaix, F., Nicolas, J.F., Cossu, G., Buckingham, M.E., 2006. Smooth muscle of the dorsal aorta shares a common clonal origin with skeletal muscle of the myotome. Development 133, 737–749.

ffrench-Constant, C., Hynes, R.O., 1989. Alternative splicing of fibronectin is temporally and spatially regulated in the chicken embryo. Development 106, 375–388.

ffrench-Constant, C., Van de Water, L., Dvorak, H.F., Hynes, R.O., 1989. Reappearance of an embryonic pattern of fibronectin splicing during wound healing in the adult rat. J. Cell Biol. 109, 903–914.

Fukuda, T., Yoshida, N., Kataoka, Y., Manabe, R., Mizuno-Horikawa, Y., Sato, M., Kuriyama, K., Yasui, N., Sekiguchi, K., 2002. Mice lacking the EDB segment of fibronectin develop normally but exhibit reduced cell growth and fibronectin matrix assembly in vitro. Cancer Res. 62, 5603–5610.

George, E.L., Georges-Labouesse, E.N., Patel-King, R.S., Rayburn, H., Hynes, R.O., 1993. Defects in mesoderm, neural tube and vascular development in mouse embryos lacking fibronectin. Development 119, 1079–1091.

George, E.L., Baldwin, H.S., Hynes, R.O., 1997. Fibronectins are essential for heart and blood vessel morphogenesis but are dispensable for initial specification of precursor cells. Blood 90, 3073–3081.

Georges-Labouesse, E.N., George, E.L., Rayburn, H., Hynes, R.O., 1996. Mesodermal development in mouse embryos mutant for fibronectin. Dev. Dyn. 207, 145–156.

Glukhova, M.A., Frid, M.G., Shekhonin, B.V., Vasilevskaya, T.D., Grunwald, J., Saginati, M., Koteliansky, V.E., 1989. Expression of extra domain A fibronectin sequence in vascular smooth muscle cells is phenotype dependent. J. Cell Biol. 109, 357–366.

Gu, H., Zou, Y.R., Rajewsky, K., 1993. Independent control of immunoglobulin switch recombination at individual switch regions evidenced through Cre-loxP-mediated gene targeting. Cell 73, 1155–1164.

Guan, J.L., Hynes, R.O., 1990. Lymphoid cells recognize an alternatively spliced segment of fibronectin via the integrin receptor alpha 4 beta 1. Cell 60, 53–61.

Guan, J.L., Trevithick, J.E., Hynes, R.O., 1990. Retroviral expression of alternatively spliced forms of rat fibronectin. J. Cell Biol. 110, 833–847.

Hashimoto-Uoshima, M., Yan, Y.Z., Schneider, G., Aukhil, I., 1997. The alternatively spliced domains EIIIB and EIIIA of human fibronectin affect cell adhesion and spreading. J. Cell Sci. 110 (Pt 18), 2271–2280.

Hynes, R.O., 1990. Fibronectins. Springer-Verlag, New York.

Hynes, R.O., 2002. Integrins: bidirectional, allosteric signaling machines. Cell 110, 673–687.

Hynes, R.O., Zhao, Q., 2000. The evolution of cell adhesion. J. Cell Biol. 150, F89–F96.

Kaspar, M., Zardi, L., Neri, D., 2006. Fibronectin as target for tumor therapy. Int. J. Cancer 118, 1331–1339.

Kornblihtt, A.R., Vibe-Pedersen, K., Baralle, F.E., 1984a. Human fibronectin: cell specific alternative mRNA splicing generates polypeptide chains differing in the number of internal repeats. Nucleic Acids Res. 12, 5853–5868.

Kornblihtt, A.R., Vibe-Pedersen, K., Baralle, F.E., 1984b. Human fibronectin: molecular cloning evidence for two mRNA species differing by an internal segment coding for a structural domain. EMBO J. 3, 221–226.

Kornblihtt, A.R., Umezawa, K., Vibe-Pedersen, K., Baralle, F.E., 1985. Primary structure of human fibronectin: differential splicing may generate at least 10 polypeptides from a single gene. EMBO J. 4, 1755–1759.

Lauffenburger, D.A., Horwitz, A.F., 1996. Cell migration: a physically integrated molecular process. Cell 84, 359–369.

Li, S., Wang, D.Z., Wang, Z., Richardson, J.A., Olson, E.N., 2003. The serum response factor coactivator myocardin is required for vascular smooth muscle development. Proc. Natl. Acad. Sci. U. S. A. 100, 9366–9370.

Liao, Y.F., Gotwals, P.J., Koteliansky, V.E., Sheppard, D., Van De Water, L., 2002. The EIIIA segment of fibronectin is a ligand for integrins alpha 9beta 1 and alpha 4beta 1 providing a novel mechanism for regulating cell adhesion by alternative splicing. J. Biol. Chem. 277, 14467–14474.

Lubarsky, B., Krasnow, M.A., 2003. Tube morphogenesis: making and shaping biological tubes. Cell 112, 19–28.

Manabe, R., Oh-e, N., Sekiguchi, K., 1999. Alternatively spliced EDA segment regulates fibronectin-dependent cell cycle progression and mitogenic signal transduction. J. Biol. Chem. 274, 5919–5924.

Marsden, M., DeSimone, D.W., 2001. Regulation of cell polarity, radial intercalation and epiboly in *Xenopus*: novel roles for integrin and fibronectin. Development 128, 3635–3647.

Marsden, M., DeSimone, D.W., 2003. Integrin-ECM interactions regulate cadherin-dependent cell adhesion and are required for convergent extension in *Xenopus*. Curr. Biol. 13, 1182–1191.

Matter, C.M., Schuler, P.K., Alessi, P., Meier, P., Ricci, R., Zhang, D., Halin, C., Castellani, P., Zardi, L., Hofer, C.K., et al., 2004. Molecular imaging of atherosclerotic plaques using a human antibody against the extra-domain B of fibronectin. Circ. Res. 95, 1225–1233.

Muro, A.F., Chauhan, A.K., Gajovic, S., Iaconcig, A., Porro, F., Stanta, G., Baralle, F.E., 2003. Regulated splicing of the fibronectin EDA exon is essential for proper skin wound healing and normal lifespan. J. Cell Biol. 162, 149–160.

Nagy, A., Vintersten, K., Behringer, R., 2003. Manipulating the Mouse Embryo: A Laboratory Manual. Cold Spring Harbor Laboratories Press, Plainview, NY.

Nilsson, F., Kosmehl, H., Zardi, L., Neri, D., 2001. Targeted delivery of tissue factor to the ED-B domain of fibronectin, a marker of angiogenesis, mediates the infarction of solid tumors in mice. Cancer Res. 61, 711–716.

Okamura, Y., Watari, M., Jerud, E.S., Young, D.W., Ishizaka, S.T., Rose, J., Chow, J.C., Strauss III, J.F., 2001. The extra domain A of fibronectin activates Toll-like receptor 4. J. Biol. Chem. 276, 10229–10233.

Oyama, F., Hirohashi, S., Shimosato, Y., Titani, K., Sekiguchi, K., 1989. Deregulation of alternative splicing of fibronectin pre-mRNA in malignant human liver tumors. J. Biol. Chem. 264, 10331–10334.

Pankov, R., Yamada, K.M., 2002. Fibronectin at a glance. J. Cell Sci. 115, 3861–3863.

Peters, J.H., Hynes, R.O., 1996. Fibronectin isoform distribution in the mouse. I. The alternatively spliced EIIIB, EIIIA, and V segments show widespread codistribution in the developing mouse embryo. Cell Adhes. Commun. 4, 103–125.

Peters, J.H., Ginsberg, M.H., Case, C.M., Cochrane, C.G., 1988. Release of soluble fibronectin containing an extra type III domain (ED1) during acute pulmonary injury mediated by oxidants or leukocytes in vivo. Am. Rev. Respir. Dis. 138, 167–174.

Peters, J.H., Chen, G.E., Hynes, R.O., 1996. Fibronectin isoform distribution in the mouse. II. Differential distribution of the alternatively spliced EIIIB, EIIIA, and V segments in the adult mouse. Cell Adhes. Commun. 4, 127–148.

Rahman, S., Patel, Y., Murray, J., Patel, K.V., Sumathipala, R., Sobel, M., Wijelath, E.S., 2005. Novel hepatocyte growth factor (HGF) binding domains on fibronectin and vitronectin coordinate a distinct and amplified Met-integrin induced signalling pathway in endothelial cells. BMC Cell Biol. 6, 8.

Schwartz, M.A., Schaller, M.D., Ginsberg, M.H., 1995. Integrins: emerging paradigms of signal transduction. Annu. Rev. Cell Dev. Biol. 11, 549–599.

Schwarzbauer, J.E., Patel, R.S., Fonda, D., Hynes, R.O., 1987. Multiple sites of alternative splicing of the rat fibronectin gene transcript. EMBO J. 6, 2573–2580.

Senger, D.R., Destree, A.T., Hynes, R.O., 1983. Complex regulation of fibronectin synthesis by cells in culture. Am. J. Physiol. 245, C144–C150.

Serini, G., Bochaton-Piallat, M.L., Ropraz, P., Geinoz, A., Borsi, L., Zardi, L., Gabbiani, G., 1998. The fibronectin domain ED-A is crucial for myofibroblastic phenotype induction by transforming growth factor-beta1. J. Cell Biol. 142, 873–881.

Shekhonin, B.V., Guriev, S.B., Irgashev, S.B., Koteliansky, V.E., 1990. Immunofluorescent identification of fibronectin and fibrinogen/fibrin in experimental myocardial infarction. J. Mol. Cell. Cardiol. 22, 533–541.

Tan, M.H., Sun, Z., Opitz, S.L., Schmidt, T.E., Peters, J.H., George, E.L., 2004. Deletion of the alternatively spliced fibronectin EIIIA domain in mice reduces atherosclerosis. Blood 104, 11–18.

Trachsel, E., Kaspar, M., Bootz, F., Detmar, M., Neri, D., 2007. A human mAb specific to oncofetal fibronectin selectively targets chronic skin inflammation in vivo. J. Invest. Dermatol. 127, 881–886.

Trinh, L.A., Stainier, D.Y., 2004. Fibronectin regulates epithelial organization during myocardial migration in zebrafish. Dev. Cell 6, 371–382.

Whittaker, C.A., Bergeron, K.F., Whittle, J., Brandhorst, B.P., Burke, R.D., Hynes, R.O., 2006. The echinoderm adhesome. Dev. Biol. 300, 252–266.

Wierzbicka-Patynowski, I., Schwarzbauer, J.E., 2003. The ins and outs of fibronectin matrix assembly. J. Cell Sci. 116, 3269–3276.

Wijelath, E.S., Murray, J., Rahman, S., Patel, Y., Ishida, A., Strand, K., Aziz, S., Cardona, C., Hammond, W.P., Savidge, G.F., et al., 2002. Novel vascular endothelial growth factor binding domains of fibronectin enhance vascular endothelial growth factor biological activity. Circ. Res. 91, 25–31.

Xia, P., Culp, L.A., 1994. Adhesion activity in fibronectin's alternatively spliced domain EDa (EIIIA) and its neighboring type III repeats: oncogene-dependent regulation. Exp. Cell Res. 213, 253–265.